Journal of Alloys and Compounds 505 (2010) 527–533

Contents lists available at ScienceDirect

Journal of Alloys and Compounds

journal homepage: www.elsevier.com/locate/jallcom

Phase transformation studies on YSZ doped with alumina. Part 1: Metastable phases

S. Nazarpour[a,*], C. López-Gándara[b], F.M. Ramos[b], A. Cirera[a]

[a] MIND/IN2UB, Departament d'Electrònica, Universitat de Barcelona, Martí i Franquès 1, Barcelona 08028, Spain
[b] FAE – Francisco Albero S.A. Rafael Barradas 19, L'Hospitalet de Llobregat 08908, Spain

ARTICLE INFO

Article history:
Received 8 March 2010
Received in revised form 17 May 2010
Accepted 28 May 2010
Available online 8 June 2010

Keywords:
YSZ
Tetragonal
Metastable phases
Alumina segregation

ABSTRACT

The goal of this study is to clarify the effect of the addition of Al_2O_3 on the grain boundaries of yttria stabilized zirconia using high resolution transmission electron microscopy. Basically excessive concentration of alumina, which is not solved in YSZ, segregates within YSZ matrix. Alumina segregates as grains between YSZ grains and as particles within YSZ grain boundaries.

t' metastable phase was detected within the grains of the sintered YSZ powders. By adding alumina into the primary YSZ powders and sintering it all together, metastable tetragonal phases appear in the grain boundaries between YSZ and segregated alumina grains. Similar phenomenon was detected in the boundaries of the two neighboring grains of YSZ doped with Alumina. Appearance of these phases might be due to the accumulated strain energies which are generated because of the alumina segregation into grain boundaries and matrix of YSZ. Hence, by controlling the dopant concentration, it could be possible to form YSZ structured by t' metastable phase. Fabrication of this material is in the great attention of the high temperature applications due to the high resistive properties of the t' metastable phase against high temperature degradation of the YSZ.

1. Introduction

Technological use of pure zirconia as a structural material is suppressed by spontaneous tetragonal to monoclinic phase transition. This transformation occurs during cooling from elevated temperature. Large destructive volume change occurs due to this phase transformation. Therefore, any application of zirconia requires cubic or tetragonal phase which are stable at room temperature. Zirconia is mostly stabilized by addition of alkaline earth or rare earth oxides. Lower dopant concentrations stabilize tetragonal phase while larger concentrations are required for cubic phase to become stable. The tetragonal phase could be formed by three methods; (1) annealing in the tetragonal stability regime (2) precipitating from cubic phase, and (3) cubic to tetragonal displacive transformation. The first two methods lead to the formation of tetragonal phase which is not favorable. In fact, tetragonal phase is metastable at low temperatures and transforms into monoclinic phase when it undergoes a stress induce transformation in the immediate vicinity of a crack tip. This transformation enhances the toughness by the well known transformation toughening mechanism. Therefore, transformation toughening is responsible for the volume change and pseudoplasticity when tetragonal phase (t) transforms into monoclinic [1,2].

The propensity to this transformation depends upon the grain size of tetragonal phase; the larger the grain size, the greater is the tendency to transform. Therefore, the grain size must be carefully controlled to prevent this transformation. The critical grain size above which spontaneous transformation occurs depends upon the dopant type and concentration.

The third way introduces metastable tetragonal phase (t') which is formed by a cubic to tetragonal transformation (ferroelastic transformation). Previously, Yashima et al. [3] showed that tetragonal YSZ can be classified into three forms, t, t', and t'', and all three forms belong to the $P4_2/nmc$ space group [4] where t corresponds to tetragonal phase. The high temperature cubic phase may also transform martensitically into metastable tetragonal phases (t' and t''). The axial ratio $c/(a\sqrt{2})$ (tetragonality) of the t and t' phase is larger than unity. These phases appear due to oxygen displacement along c-axis [4]. The axial ratio equal to unity has been seen in t'' phase. This phase has the dimensionality of a cubic phase with a tetragonal symmetry. Therefore, it is extremely difficult to distinguish t'' phase from cubic one by TEM images. In fact, t'' phase as well as t' phase appears due to the oxygen displacement along lattice c-axis [4–7]. Crystallographically, the t' phase is identical with the t phase; however, its morphology is quite different. The t' phase consists of extremely fine domains which makes this phase highly resistant to martensitic transformation. In t' phase materials, therefore, it is not

* Corresponding author. Tel.: +34 934037094.
E-mail addresses: snazarpour@ub.edu, nazarpour@ub.edu (S. Nazarpour).

0925-8388/$ – see front matter © 2010 Elsevier B.V. All rights reserved.
doi:10.1016/j.jallcom.2010.05.136

the grain size that matters insofar as martensitic transformation is concerned, but the critical parameter is the domain size. Since the cubic phase is stable at elevated temperatures, the formation of t' phase requires that the temperature be raised high enough. Treatment at high temperatures is not favorable for technological process doe to the extra costs and production time. Therefore, it would be entirely interesting to form t' phase without modifying the fabrication process of the device. In this study, we study the generation of t' metastable phase as a consequence of YSZ oversaturation by alumina. Since oversaturation of alumina results in large accumulated strain energy in YSZ matrix, martensitic transformation may occur. By this transformation, cubic or tetragonal phases of YSZ transforms into t' phase. There are numerous reports in the literature concerning the effect of alumina on ameliorating the weak mechanical properties of YSZ. Previously, effective role of Al_2O_3 on decreasing the sintering temperature of CaO-stabilized ZrO_2 were studied by Beekmans and Heyne [8]. They showed that alumina enhances the mechanical properties of YSZ. This enhancement in mechanical properties might be limited because of the limited solubility of alumina into zirconia. There are reports in the literature which indicate that the solubility of Al_2O_3 into ZrO_2 is quite limited [9–11]. However higher solubility of alumina into zirconia has been reported by Stough and Hellmann [12]. Basically, addition of the Al_2O_3 into ZrO_2 within solubility limit slightly increases the bulk resistivity and dramatically increases the resistivity of the grain boundaries [9]. Extra addition of Al_2O_3 above solubility limit until 5 wt% increases the bulk resistivity and reduces the resistivity of the grain boundaries [13,14]. Excessive addition of Al_2O_3 more than 5 wt% brings about further increase in the bulk and grain boundary resistivity [15–17]. It has been found that oversaturated Al_2O_3 segregates [9] and forms precipitates predominantly at grain boundaries [18,19], but also reportedly within the ZrO_2 grains. Hence, variation of electrical resistivity of zirconia could be considered as a consequence of alumina segregation [20–22]. Theoretically, residual stress which arises due to the alumina segregation modulates the electrical resistivity. The relation between electrical resistivity, residual stress, and alumina segregation is discussed partly in this article and the next article (part 2) as well.

2. Experimental procedure

Two series of specimens were sintered at 1450 °C for 3 h. First one consists of zirconia with 4.5 mol% Y_2O_3 (YSZ) and the second is zirconia with 4.5 mol% Y_2O_3 and 9.4 mol% Al_2O_3 (YSZ-Al). Further details on sintering process are given by López-Gándara et al. [23]. The crystalline structure was determined by X-Ray Diffraction (XRD) analyses in θ–2θ scan by means of a 4-circle X-ray diffractometer with Cu-Kα radiation (MRD PHILIPS) and high accuracy XRD (Pananalytical) to analyze in θ–2θ scan mode from 70° to 80°. Raman spectrometry (Jobin Yvon T64000) with a visible Ar^+ laser has been used to investigate the zirconia tetragonal crystals. The microstructure was examined by Scanning Electron Microscopy (SEM) (ESEM Quanta 200 FEI), Transmission Electron Microscopy (TEM) (Hitachi 800MT, 300 kV) and High Resolution Transmission Electron Microscopy (HRTEM) (JEOL JEM 2100, 200 kV). Besides, nanoprobe Energy Dispersive Spectroscopy (EDS) was used to investigate the segregation of the dopants into the grain boundaries. The nanoprobe EDS measurement were performed with probe size of 0.5 nm at every 1 nm across the grain boundaries.

Specimens for TEM observations were prepared via conventional preparation techniques, polishing, dimple grinding, and ion milling to obtain electron transparency.

3. Results and discussion

Fig. 1 corresponds to XRD diffractions of YSZ without alumina (sample 1) and YSZ doped with 9.4 mol% Al_2O_3 (sample 2). It is well known that 4.5 mol% yttria partially stabilizes tetragonal phase and sintered material is a mix of cubic and tetragonal phases. Presence of (4 0 0) crystal diffraction at 2θ equal to 74° confirms the existence of cubic phase [24]. Tetragonal phase was detected as well by the presence of six active modes in Raman spectra (not shown).

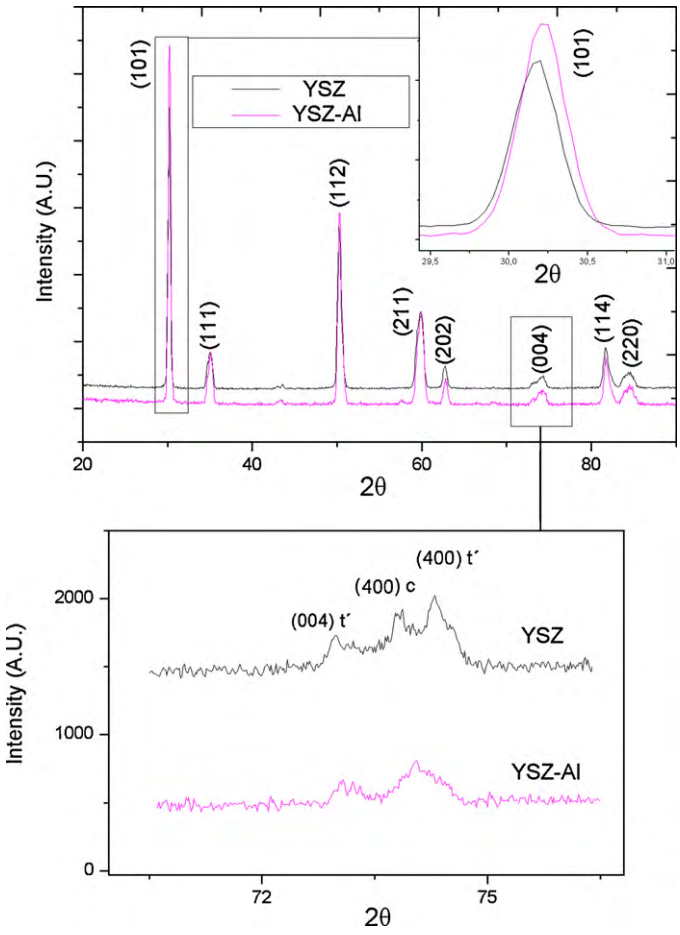

Fig. 1. XRD results of YSZ and YSZ-Al. The shifting of the (1 0 1) diffraction is noticeable.

No monoclinic phase was detected from XRD and Raman results. In the second sample, by adding alumina into YSZ, 2θ positions in the intense (1 0 1) diffraction peak shifted toward higher degrees. Simply, it could be concluded that by adding alumina into YSZ, spacing between YSZ-Al (1 0 1) planes became smaller in comparison with YSZ (1 0 1) planes. Esquivias et al. [25] showed that shifting of the ZrO_2 main diffraction peak toward higher 2θ might be due to partially transition of the tetragonal phase to metastable ones. Hence, electron microscopy was used to reveal the phase transition in the grain boundaries of the samples. Alumina diffraction peaks were not detected because of its low concentration in comparison with YSZ.

Fig. 2(A) presents the TEM images of YSZ sample. There is no clue for any segregation of yttria. In the second sample, by adding alumina into YSZ, the grain size is roughly in the same order of the first sample (YSZ) (Fig. 2(B)). This reveals that in these samples, any effect of the grain size on the metastable phase transformation is negligible.

Fig. 2(C) presents the TEM image of the second sample (YSZ-Al). Fast Fourier transform (FFT) of the shiny particles confirmed that they are alumina grains that segregate within the host matrix.

By taking into account that alumina particles initially segregate in the grain boundaries of YSZ-Al [9,18,19], grain boundaries were studied using HRTEM. Fig. 3(A) and (B) presents the HRTEM images of YSZ (sample 1) and YSZ-Al (sample 2), respectively. Fig. 3(A) shows two neighboring grains of YSZ and the grain boundary between them. Neighboring grains are labeled with (a) and (c) while the grain boundary in between is marked (b). FFT image of grain (a) shows different diffractions with d-spacing between

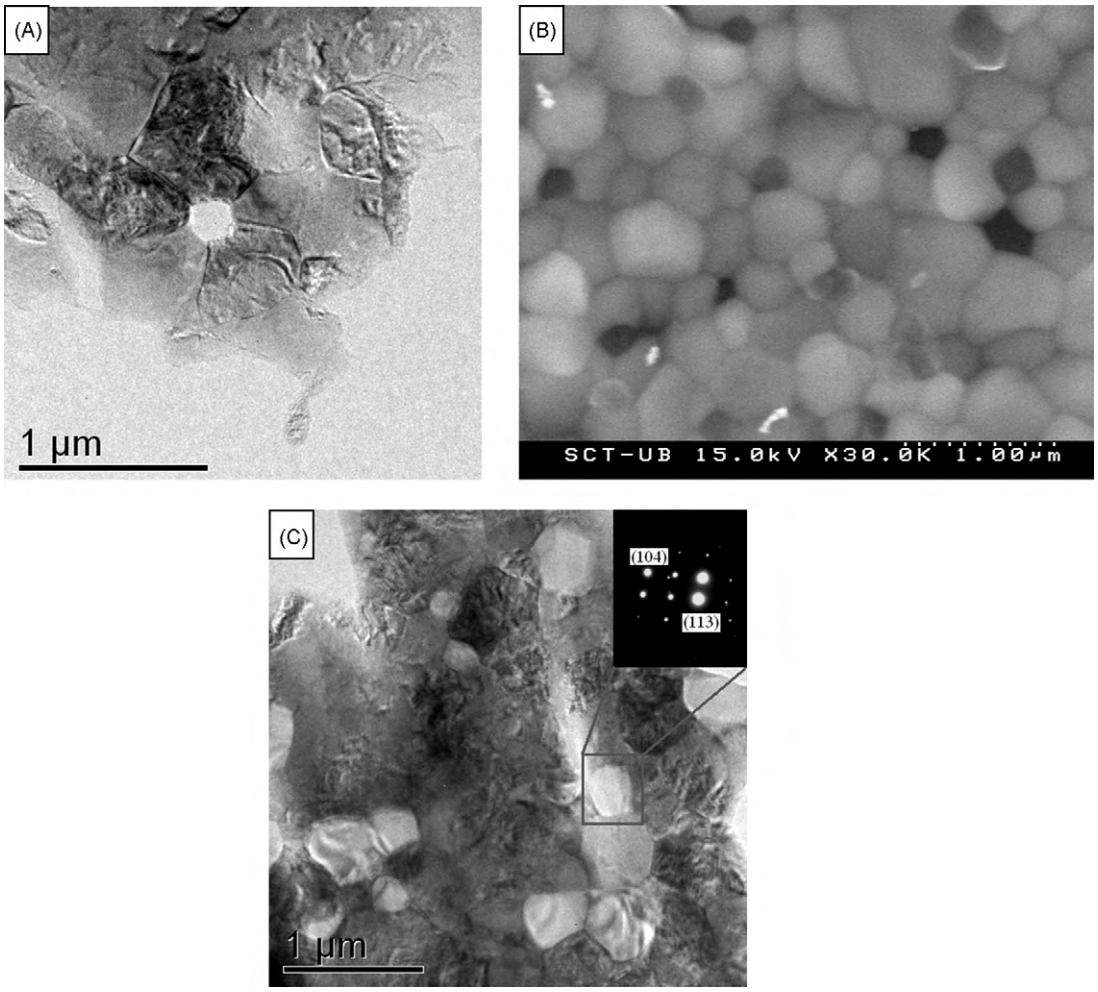

Fig. 2. TEM image of YSZ (A), SEM image of YSZ-Al (B), TEM image of YSZ-Al (C). SAED of a Shiny grain of YSZ-Al (right top image in (C)) confirmed that these grains are segregated alumina.

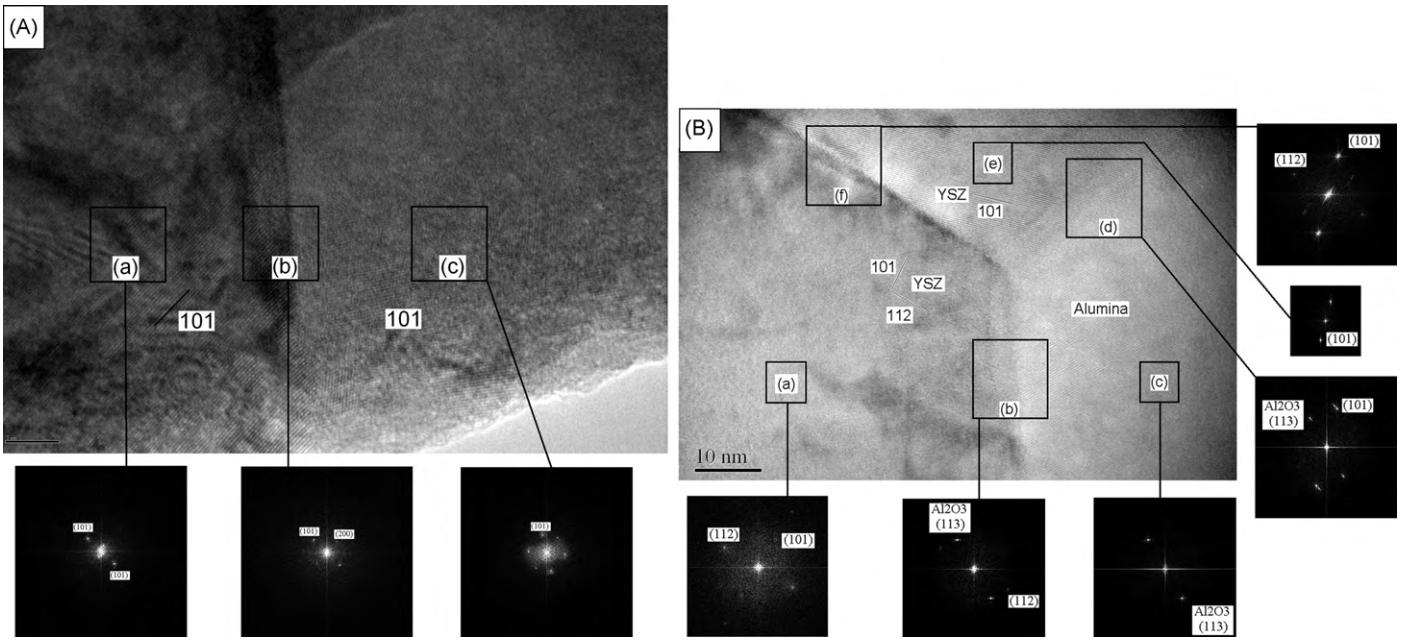

Fig. 3. HRTEM images of YSZ (A) and YSZ-Al (B). Three different areas of YSZ (A) were analyzed which are two neighboring grains (a) and (c), and the grain boundary between them (b). HRTEM image of YSZ-Al (A) consists of several regions as well which are described in the text. It contains YSZ grains (a) and (e), segregated alumina grain (c), the boundaries between YSZ grains (f), and the boundaries between YSZ and alumina grain (b) and (d). Corresponding FFT image of each region was obtained and metastable phases were detected in the grains of YSZ and in the boundaries of YSZ-Al.

2.7113 Å and 2.9885 Å. These values correspond to (1 0 1) tetragonal YSZ plane ($2\theta = 30.135^\circ$ in XRD results). Theoretically, the spacing between each plane should be a constant value. Hence, the presence of t' phase inside the grain (a) may be suggested because of the second value of d-spacing. In fact, the d-spacing of (1 0 1) tetragonal YSZ plane shows the value of *c*-axis of the lattice. In the other words, two different values of d-spacing present two different *c*-axes. From a crystallographic point of view, the ratio of the cell parameters can be used to distinguish between the two tetragonal phases (t and t'). Since evaluation of tetragonality by means of Bragg's law may face with accuracy problems, variation of d-spacing of lattices could be an appropriate way for evaluation of the dimensions of the lattice. Hence, FFT spots in the vicinity of the main (1 0 1) spots confirm the appearance of metastable phases with dissimilar d-spacing than tetragonal. Basically one of the diffractions confirms that *c* parameter of the lattice became smaller and therefore, t' phase may appear. The reason for the existence of tetragonal lattices with different d-spacing might be owing to irregular distribution of yttria within the matrix. In fact, it could be possible that yttria has not been solved homogeneously in the zirconia lattices. Therefore, some lattices may contain lower concentration of yttria than 4.5 mol%. This results in a second phase with higher tetragonality. It should be noted that by increasing the concentration of yttria, *c* parameter of the lattice decreases (lower tetragonality). As mentioned before, due to the partially stabilizing the zirconia by yttria, cubic phase is presented in YSZ sample as well as tetragonal phase. However, cubic phase was not detected in region (a) of Fig. 3(A).

The structure of grain (c) consists of a perfect t phase lattice with (1 0 1) direction. However, the lattices of region (b) which is the grain boundary between grains (a) and (c), is a mix of cubic and tetragonal whereas there is no clue for existence of t' phase.

Fig. 3(B) presents the HRTEM images of a triple grain boundary. This boundary is between two YSZ-Al grains (a) and (e) and an alumina segregated grain (c). FFT results of grain (a) shows the (1 0 1) t and (1 1 2) t plane. Since the structure of another YSZ-Al grain (e) is (1 0 1) t, it could be concluded that the structure of these grains is fully tetragonal. This finding has been checked out in different grains and fairly comparable results have been seen, although cubic phase was detected in some grains of YSZ-Al.

It should be noted that the structure of the grains of YSZ sample consists of t and t', whereas by adding alumina it became fully tetragonal. Furthermore, FFT results of the grain boundary (b) between YSZ grain (a) and alumina segregated grain (c) shows the presence of t, t', and alumina. Therefore, by comparing FFT images of region (a)–(c), presence of t' phase in the boundaries would be confirmed. Comparable phenomenon occurred in the region (d). Grain boundary (d) contains t' metastable phase while there is no t' phase inside the grain structures.

Essentially, YSZ-Al samples made of two kinds of grain boundaries; one is the boundary between YSZ grains and the other is the boundary between YSZ and Alumina grains. The grain boundaries made by alumina grains are all comparable, including triple grain boundaries. However, the grain boundaries (f) between two YSZ neighboring grains (a) and (e) contain t, t', and cubic lattices. There is no way to distinguish t'' from cubic structure with FFT diffractions since their lattice dimensions are equal.

The reason for the appearance of tetragonal metastable phases might be the segregation of alumina into the grain boundaries. In fact, alumina and yttria dissolve in zirconia similarly though the interstitial dissolving of alumina is energetically unfavorable [26]. Therefore, higher concentration of alumina most likely leads to an increase in the oxygen vacancy in the vicinity of the grain boundaries whereas transformation of the t phase to t', t'', and cubic phase may happen. Previously, Balmer et al. [27] proposed high solubility limit (up to 40 wt%) of alumina into metastable tetragonal zirconia. This high solubility limit appears because by addition of alumina into the structure, d-spacing of the lattice will be increased. Therefore, metastable phase may transform to the tetragonal phase which is energetically stable. Phases in each area were mentioned as well in Table 1.

Table 1
Phases which constructed out the grains and grain boundaries of YSZ and YSZ-Al, obtained by HRTEM.

Figure	(a)	(b)	(c)	(d)	(e)	(f)
3(A)	$t+t'$	t + cubic	t	–	–	–
3(B)	t	$t+t'$ + Al	Al	$t+t'$ + Al	t	$t+t'$

The obtained FFT results may not be able to distinguish accurately the crystal direction of the grain boundaries due to possible overlapping of the crystallographic planes of neighboring grains in the vicinity of the grain boundaries. Therefore, Selected Area Electron Diffraction (SAED) analysis was carried out obtaining diffraction of the two neighboring grains and their boundary in between (Fig. 4(A)). It should be noted that the SAED analyzing area is not the same as Fig. 3. This may help to achieve better statistics on the obtained results. By patterning the lattice of each grain (numbers 1 and 2 in Fig. 4(A)) and superimposing them onto the last SAED image (number 3 in Fig. 4(A)), a pattern will remain. Remained pattern could roughly illustrate the main crystal direction of the grain boundary without overlapping of the neighboring grains. Fig. 4(B) shows the SAED of the first neighboring grain of YSZ sample (sample 1). The shiny dots are equal to 2.778 Å and 2.140 Å which are related to (1 0 1) and (1 0 2) crystal directions, respectively. As shown with circles in Fig. 4(B), two shiny diffractions are found with small difference in d-spacing. This proves that metastable tetragonal phases appear in the matrix of tetragonal grain. Therefore, this grain is constructed by t and t' phase. In addition, there is no clue for existence of cubic phase in this grain. Other neighboring grain showed tetragonal and cubic phase. Since the analyzing area of the SAED is wider than width of the grain boundaries, a mix of two neighboring grains and grain boundary has been captured (Fig. 4(C)). Circles in Fig. 3(B) are the remained SAED pattern of YSZ sample (sample 1) after superimposing process. Hence, remained pattern corresponds to the planes of YSZ grain boundary with 2.088 Å, 1.218 Å, and 1.188 Å d-spacing. Thus, one could be concluded is that 2.021 Å d-spacing corresponds to (1 0 2) t phase. Besides, 1.218 Å is the d-spacing of the cubic (0 0 4) planes. Therefore, it could be suggested that in YSZ sample, the structure of the grains are t, t', and cubic phase, and the grain boundaries mostly consists of cubic + t phase. The similar process has been done in different areas of YSZ and the results were coherent. Obtained results are in agreement with Table 1.

Fig. 4(D) and (E) is the SAED of the grain and grain boundary of YSZ-Al sample (sample 2), respectively. These grains are both YSZ and no alumina grain was considered. Fig. 4(D) shows the first neighboring grain with (1 1 2) planes. The other neighboring grain consists of tetragonal and cubic phase with 1.433 Å d-spacing. After reducing the pattern of two neighboring grains from SAED of YSZ-Al grain boundary, perfect cubic diffraction has been seen, showed by circles in Fig. 4(E). However, rectangles in Fig. 4(E) show the presence of metastable phases in the grain boundary. Once again, the attendance of two side by side diffraction spots illustrates the presence of metastable phase with slight variation in d-spacing which corresponds to t and t' phase. However, during superimposing the spots, tetragonal diffraction spots may diminish in large portion because the d-spacing of the tetragonal phase in the neighboring grain is equal to the d-spacing of the tetragonal phase in the grain boundary. Hence, during the superimposing process, a number of diffraction spots will be filtered which is due to the diffraction of

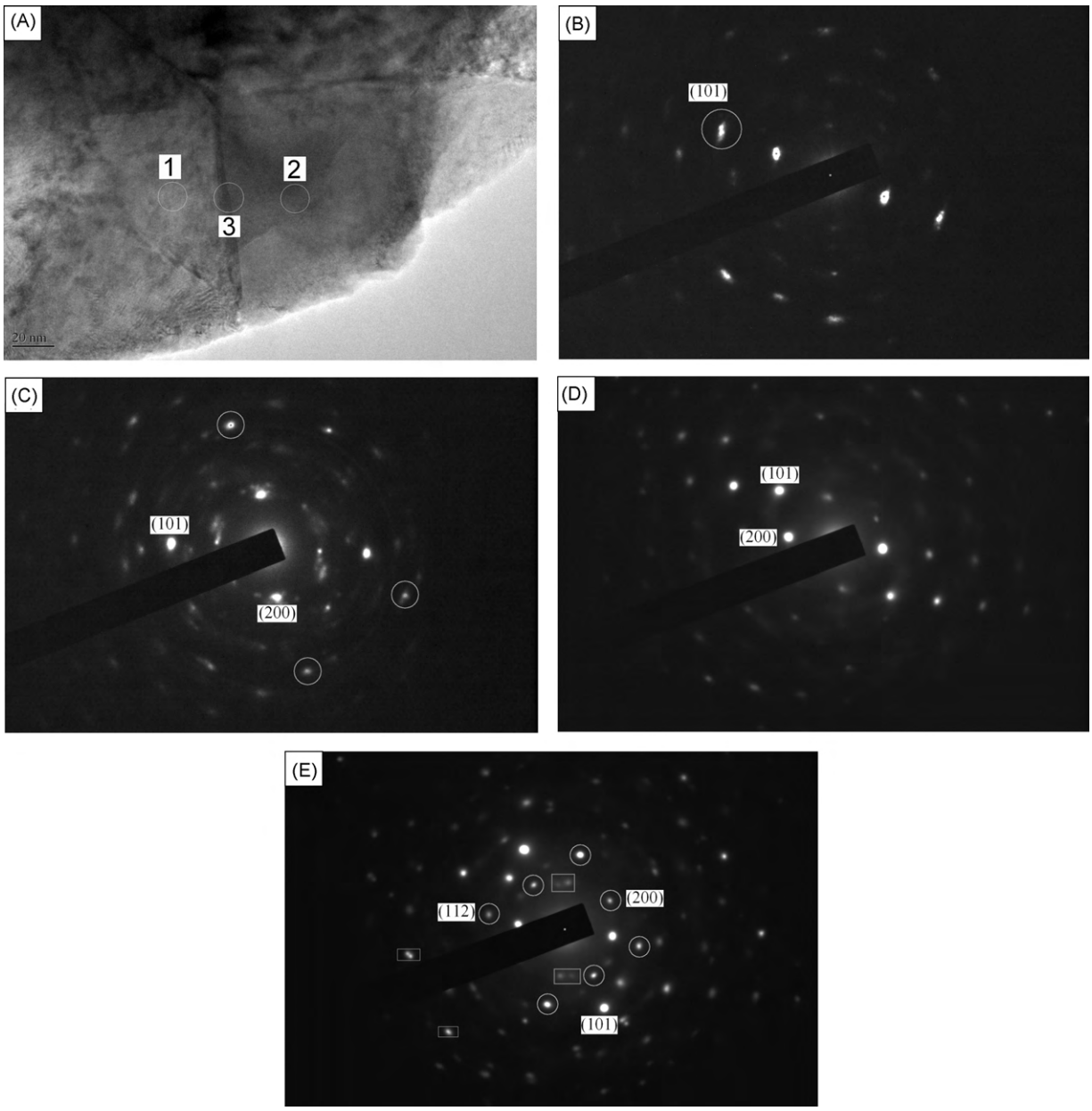

Fig. 4. The selected areas for electron diffraction are identical with circles in (A). Area with numbers 1 and 3 are related to two neighbouring grains whereas area with number 2 corresponds to the two neighbouring grains with grain boundary between them. SAED of the YSZ neighboring grain (B), YSZ grain boundary (C), YSZ-Al neighboring grain (D), YSZ-Al grain boundary (E) were presented.

second neighboring grain. This is the reason that different diffraction spots are not presented in these images.

Metastable phases mostly present in the grain boundaries of YSZ-Al (sample 2). Table 2 shows the existed phases in YSZ and YSZ-Al using SAED analysis. These results are comparable with Table 1 and the only difference is related to YSZ grains in sample 1 and the phases in the grain boundaries of YSZ-Al (sample 2). This difference probably is due to the dissimilar analyzing area of HRTEM and SAED.

Table 2
Phases which constructed out the grains and grain boundaries of YSZ and YSZ-Al, obtained by SAED.

Sample	YSZ grain 1	YSZ–YSZ grain boundary	YSZ grain 2
YSZ	$t + t'$	$t + c$	t
YSZ-Al	t + cubic	$t + t'$ + cubic	t

Additionally, Matsui et al. [28] showed the presence of cubic region in YSZ doped with alumina which forms mostly in the vicinity of the grain boundaries. However, this cubic phase may coexist with t' phase as well. In order to investigate the effect of yttria and alumina segregation, variation of yttria and alumina concentration within the grain boundaries were determined using nanorpobe EDS. Fig. 5(A) presents the typical yttria distribution profile across the grains of YSZ sample. It can be seen that yttria segregated in the YSZ grain boundaries and its concentration reaches to 7 mol%. This high concentration of yttria within grain boundaries leads to appearance of cubic phase in the boundaries of YSZ sample. This is in agreement with HRTEM and SAED results. However, it can be seen that the concentration of yttria in first neighboring grains is a little bit higher than the interior grain. Hence, presence of cubic phase in the grain structure of YSZ sample is inevitable. By comparing the results of HRTEM and EDS, it can be concluded that the appearance of t' phase is in connection with yttria segrega-

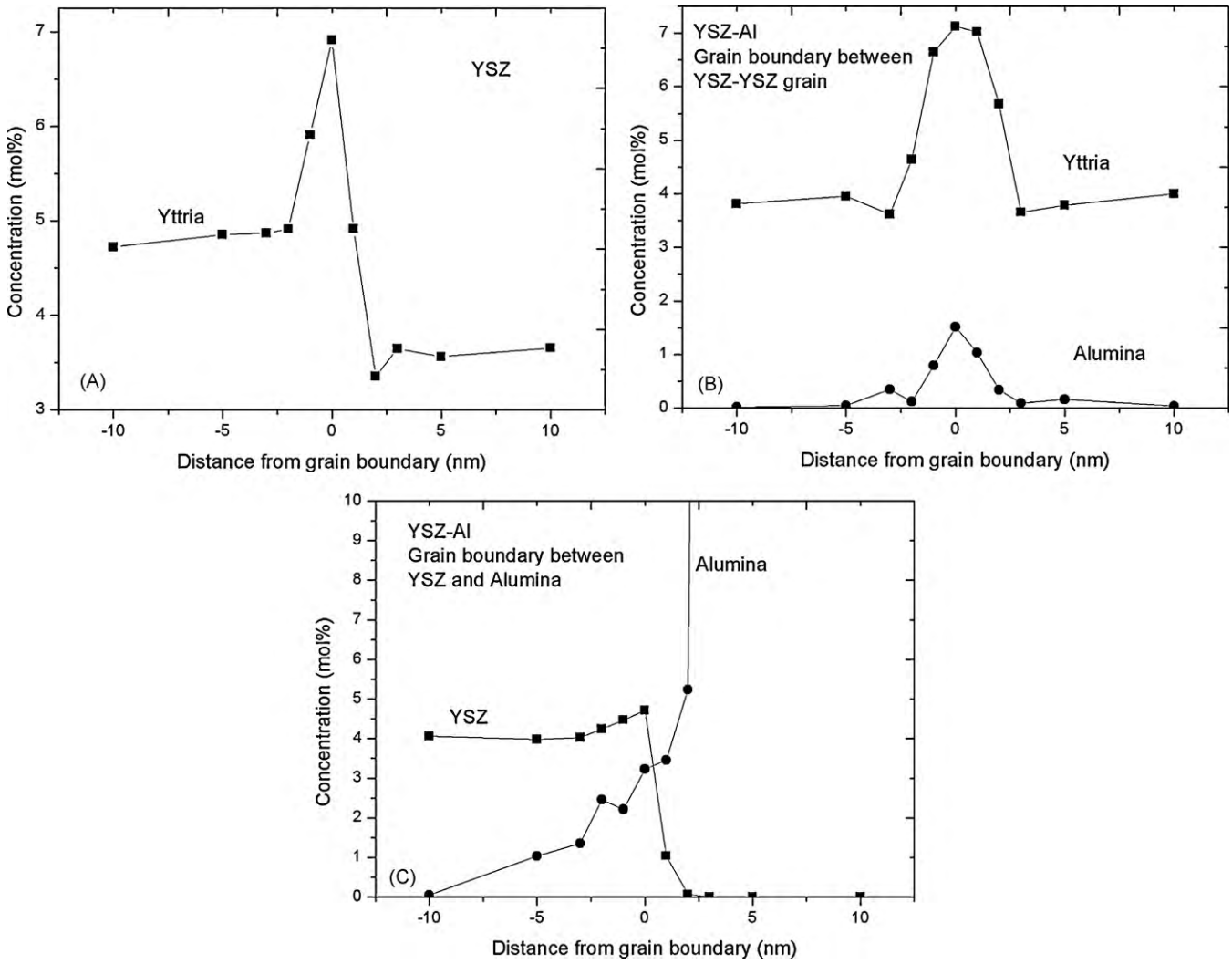

Fig. 5. YSZ and alumina concentration profile were presented in the grain boundaries of YSZ (A), and YSZ-Al (B) and (C). Segregation of yttria was detected in grain boundaries of YSZ (A). In addition concentration of yttria is slightly higher in first neighboring grain than interior one. The boundaries in YSZ-Al (B) and (C) consist of boundaries between YSZ grains (B) and the boundaries between YSZ and segregated alumina grains (C). Presence of alumina in the boundaries of YSZ-Al sample is significant which led to appearance of t' phase in the boundaries.

tion as well. Fig. 5(B) shows yttria and alumina profile across grain boundary of two YSZ grain in the YSZ-Al sample. An increase in the grain boundary length is evident in compare with YSZ sample. It can be seen that yttria and alumina segregates into the grain boundaries. In fact, alumina increases the density of the oxygen vacancy in the zirconia in the same way that yttria does. Therefore, dissolved alumina in the YSZ grain may change some metastable phases into cubic. This could be the reason that after adding alumina (YSZ-Al sample), t' phase has not been seen within YSZ grains. It is well known that the segregation of elements into the grain boundaries brings about accumulation of strain energy along the boundaries. We do believe that these stresses affect on the appearance of metastable phases inside and besides the grain boundaries due to the fact that tetragonal to metastable phase transformation is martensitic. Since the solubility limit of alumina into zirconia is entirely limited, extra alumina segregates on the grain boundaries and displaced the oxygen vacancies of the tetragonal phase which leads to appearance of metastable phases. It should be noted that in Fig. 5(B), alumina concentration profile was not equal to zero in the vicinity of the boundary. Therefore, it could be suggested that t' phase could be presented as well in the vicinity of the grain boundaries. However, it needs further studies. Furthermore, Fig. 5(C) shows the yttria and alumina concentration profile across grain boundary between YSZ and interior segregated alumina grains (Fig. 3(B), area (b) and (d)). It can be seen that yttria did not segregate into the grain boundary whereas concentration of alumina is significant. In addition, composition of yttria became negligible in the alumina grain. However, based on the obtained results from Fig. 3(B), the boundary between alumina and YSZ grains consists of t' phase. This, in turn, confirms the relation within presence of alumina and appearance of t' phase. Obtaining t' phase YSZ is extremely important in the industrial application due to their excellent resistance to destructive martensitic transformation which is common in large-grained t phase materials. Besides, its excellent toughness, good strength, and excellent creep resistance make this phase remarkable as well. Because of its properties, the t' phase material would seem to be ideally suited for elevated temperature applications such as heating elements, and the like. However, t' phase systems have been very difficult to manufacture in form that is suitable for applications. Most of the literature reported on the t' phase is either arc melted samples or in samples containing over 6 mol% yttria. Arc melted materials can only be used for microstructural characterization, which are not in a functional form for applications. The properties of the latter, high yttria content materials are not attractive. They contain t' phase with too small of a tetragonality, and have properties not much

better than the cubic phase. However, after adding alumina into YSZ, the tetragonality of the t phase decreased slightly and t' phase appeared. Besides, the principal limitation in manufacturing a t' phase zirconia with low dopant content has been the high fabrication temperatures required. However, addition of alumina leads to appearance of t' phase without any extra fabrication process. In fact, this phase appears during sintering of YSZ and alumina powders. Therefore, addition of alumina is beneficial as well for high temperature application. However, its limitation is that t' phase did not appear inside the grains. In fact, enhanced mechanical properties after addition of alumina which has been reported previously elsewhere are because of the presence of t' phase in the boundaries of YSZ.

4. Conclusion

As conclusion, it has been seen that grains of YSZ sample without alumina consists of t, t' and cubic phase while t' phase is not existed in the grain boundaries. The structure of the grains in YSZ-Al is t and cubic phase. Besides, YSZ-Al grain boundaries are mostly a mix of t, t', and cubic phases which are essentially dependent on the concentration of segregated alumina in the boundaries. Moreover, addition of alumina into YSZ caused higher concentration of cubic phases appeared in YSZ-Al grains. It could be concluded that by oversaturation of YSZ with alumina powder, over the solubility limit, t' phase appears around segregated alumina particles. It could be suggested that t' phase forms in the grain boundaries due to accumulated strain energy owing to alumina segregation. This stress affects on the appearance of metastable phases inside the grain boundaries due to the fact that tetragonal to metastable phase transformation is martensitic. Since the solubility limit of alumina into zirconia is entirely limited, extra alumina segregates on the grain boundaries and displaces the oxygen vacancies of the tetragonal phase which leads to the appearance of metastable phases. However, further study is essential to investigate the appearance of t' phase in the vicinity of grain boundaries as well as inside the boundaries.

References

[1] E.C. Subbarao, Adv. Ceram. 3 (1981) 1.
[2] W.E. Lee, W.M. Rainforth, Ceramic Microstructure, Chapman & Hall, London, 1994.
[3] M. Yashima, M. Kakihana, M. Yoshimura, Solid State Ionics 86–88 (1996) 1131.
[4] M. Yashima, S. Sasaki, M. Kakihana, Y. Yamaguchi, H. Arashi, M. Yoshimura, Acta Crystallogr. B 50 (1994) 663.
[5] M. Yashima, K. Ohtake, H. Arashi, M. Kakihana, M. Yoshimura, J. Appl. Phys. 74 (1993) 7603.
[6] M. Yashima, N. Ishizawa, M. Yoshimura, J. Am. Ceram. Soc. 76 (1993) 641.
[7] M. Yashima, N. Ishizawa, M. Yoshimura, J. Am. Ceram. Soc. 76 (1993) 649.
[8] N.M. Beekmans, L. Heyne, Electrochim. Acta 21 (1976) 303.
[9] M. Miyayma, H. Yanagida, A. Asada, Am. Ceram. Soc. Bull. 64 (1985) 660.
[10] L.M. Navarro, P. Recio, J.R. Jurado, P. Duran, J. Mater. Sci. 30 (1995) 1949.
[11] A.J. Feighey, J.T.S. Irvine, Solid State Ionics 121 (1999) 209.
[12] M.A. Stough, J.R. Hellmann, J. Am. Ceram. Soc. 85 (2002) 2895.
[13] S.P.S. Badwal, F.T. Ciacchi, S. Rajendran, J. Drennan, Solid State Ionics 109 (1998) 167.
[14] Y. Li, J. Liu, Z. Lu, X. Zhao, T. He, W. Su, Solid State Ionics 126 (1999) 277.
[15] K. Yamana, W. Weppner, A. Kopp, T. Yoshimura, J. Mater. Sci. Lett. 10 (1991) 1205.
[16] M. Fukuya, K. Hirota, O. Yamaguchi, H. Kume, S. Inamura, H. Miyamoto, N. Shiokawa, R. Shikata, Mater. Res. Bull. 29 (1994) 619.
[17] M. Mori, T. Abe, H. Itoh, O. Yamamoto, Y. Takeda, T. Kawahara, Solid State Ionics 74 (1994) 2217.
[18] G. Dotelli, R. Volpe, I. Natali-Sora, C. Marti, Solid State Ionics 113–115 (1998) 325.
[19] A. Yuzaki, A. Kishimoto, Solid State Ionics 116 (1999) 47.
[20] X. Guo, R.Z. Yuan, J. Mater. Sci. 30 (1995) 923.
[21] X. Guo, J. Am. Ceram. Soc. 86 (2003) 1867.
[22] X. Guo, C.Q. Tang, R.Z. Yuan, J. Eur. Ceram. Soc. 15 (1995) 25.
[23] C. López-Gándara, F.M. Ramos, A. Cirera, A. Cornet, Sens. Actuators B 140 (2009) 432.
[24] C. Viazzi, J.P. Bonino, F. Ansart, A. Barnabe, J. Alloy Compd. 452 (2008) 377.
[25] L. Esquivias, C. Barrera-Solano, M. Pifiero, C. Prieto, J. Alloy Compd. 239 (1996) 71.
[26] M.O. Zacate, L. Minervini, D.J. Bradfield, R.W. Grimes, K.E. Sickafus, Solid State Ionics 128 (2000) 243.
[27] M.L. Balmer, F.F. Lange, C.G. Levi, J. Am. Ceram. Soc. 77 (1994) 2069.
[28] K. Matsui, N. Ohmichi, M. Ohgai, J. Mater. Res. 21 (2006) 2278.